ISSN 1392-1207. MECHANIKA. Vol. 29, No. 2, 2023: 115–124

Vibration Drives with Two Impacting Pairs for Precise Robots

Kazimieras RAGULSKIS*, Liutauras RAGULSKIS**
**Kaunas University of Technology, K. Donelaičio st. 73, LT-44249, Kaunas, Lithuania, E-mail: kazimieras3@hotmail.com*
***Vytautas Magnus University, Vileikos st. 8, LT-44404, Kaunas, Lithuania, E-mail: l.ragulskis@if.vdu.lt*
https://doi.org/10.5755/j02.mech.32277

1. Introduction

In the field of vibrational impact systems important results of investigations have been obtained, which became widely accepted and are applied in further investigations (V. Astashov, R. Nagaev, V. Babitski, A. Kobrinski, B. Bakšys, V. Ragulskienė, R. Bansevičius, L. Bespalova, V. Metrikin, A. A. Kobrinski, V. Vekteris, J. Viba, M. Feigin, R. Bort, D. Eyle, F. Frendenstein, R. Johnson, V. Klimov, A. Shliachtin, L. Tives, T. Lieber, S. Mavri, T. Caughey, H. Neuber, V. Ostaševičius, W. Park, F. Peterka, A. Charkevich, W. Pilkey, J. Sparenberg, A. Tustin, K. Cornelius, V. Eglais, L. Eierlich).

Contemporary investigations of systems of new type with specific nonlinearities as well as with motions of chaotic type are performed.

Earlier it was shown that in some types of nonlinear systems between the hard and soft zones of excitation of vibrations optimal regimes according to the shape of motion exist. Here this fact is generalized for the vibrator with two symmetric impacting pairs of elements.

According to the model of the system free vibrations of the system and their parameters are determined as well as forced harmonic vibrations and their specific features are determined.

Systems of the investigated type are met in elements of robots. Various types of robots are investigated by V. A. Glazunov [1]. Vibratory drives are described in [2]. Resonant zones are analyzed in [3]. Theoretical basis of vibrational impact systems is described in [4]. Vibrations and impacts in transmissions are presented in [5]. Applications in the field of manipulators and robots are investigated in [6]. Resonances in nonlinear systems are described in [7]. Systems with impacts are investigated in [8]. Stabilization of dynamical systems is presented in [9]. Impacts in vibrating systems are investigated in [10]. Periodic orbits are analyzed in [11]. Vibro-impact energy sink is investigated in [12]. Particle impact with a wall is presented in [13]. Frequencies of a multibody system are analyzed in [14]. Pendulum and its dynamics are investigated in [15]. Piecewise linearity is analyzed in [16]. Resonant zones are investigated in [17]. Sommerfeld effect is presented in [18]. Isolated resonances are investigated in [19].

Recommendations for practical applications are provided.

2. Model of the system

The investigated system is shown in Fig. 1.

Differential equation of motion of the member 3 is the following one:

$$m\ddot{x} + 2H\dot{x} + 2Cx = F\sin\omega t, \text{ when } -x_s < x < x_s. \quad (1)$$

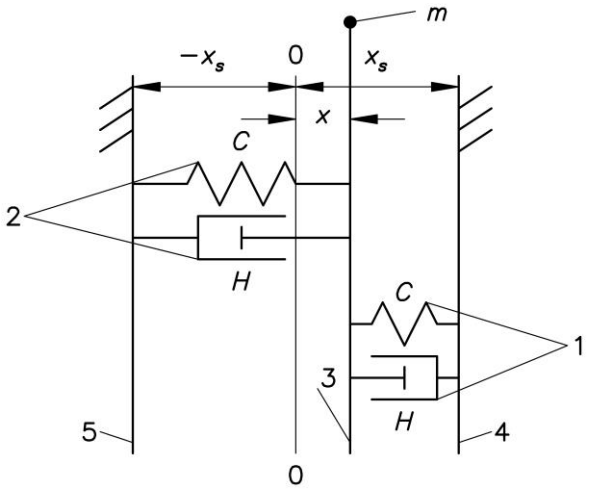

Fig. 1 *1* and *2* are springs, between them the member *3* of mass *m* is compressed and performs motion in the interval $-x_s < x < +x_s$, in the positions $x = +x_s$ and $x = -x_s$ the member *3* impacts into the immovable supports *4* and *5*; static position of equilibrium of the springs *1* and *2* is in the position $x = 0$; the coefficients of stiffness of both springs are *C* and the coefficients of damping of both dissipative members are *H*; motion of the member *3* is excited by an external force $F\sin\omega t$

The notations are introduced:

$$\tau = pt, \ \dot{} = \frac{d}{dt}, \ ' = \frac{d}{d\tau}, \ p^2 = \frac{2C}{m}, \ 2h = \frac{2H}{\sqrt{2Cm}},$$
$$\nu = \frac{\omega}{p}, \ f = \frac{F}{2C}. \quad (2)$$

The Eq. (1) by taking into account the Eq. (2) becomes the following one:

$$x'' + 2hx' + x = f\sin\nu\tau, \quad (3)$$

which is valid for $-x_s < x < +x_s$.

When $x = x_s$ and $x = -x_s$ during the collision of the member 3 with the immovable supports instantaneous impacts take place, which change the velocity of the member 3 according to the equation:

$$x'^{+} = -Rx'^{-}, \quad (4)$$

where x'^{-} denotes the velocity before impact and x'^{+} denotes the velocity after impact, *R* is the coefficient of restitution of velocity.

It is assumed that in the interval:

$$\tau \in \left(\tau_i, \tau_j\right), \tag{5}$$

impacts take place:

$$\text{at } \tau = \tau_i \text{ when } x = x_s, \text{ and at } \tau = \tau_j \text{ when } x = -x_s. \tag{6}$$

When:

$$\begin{aligned} &\tau = \tau_i - 0,\ x_i'^{-} > 0 \text{ and when} \\ &\tau = \tau_i + 0,\ x_i'^{+} = -Rx_i'^{-}, \\ &\tau = \tau_j - 0,\ x_j'^{-} < 0 \text{ and when} \\ &\tau = \tau_j + 0,\ x_j'^{+} = -Rx_j'^{-}. \end{aligned} \tag{7}$$

3. Conservative system

It is assumed that:

$$h = f = 0,\ R = 1. \tag{8}$$

The equation of motion is the following one:

$$x'' + x = 0 \text{ when } x \in \left(-x_s, x_s\right). \tag{9}$$

Motion takes place according to the two intervals $\tau \in \left(0, \tau_1\right)$ and $\tau \in \left(\tau_1, 2\tau_1\right)$, where:

$$\begin{aligned} &\text{at } \tau = 0,\ x_0 = x_s, \text{ at } \tau = \tau_1,\ x_1 = -x_s, \\ &\text{at } \tau = \tau_2,\ x_2 = x_s. \end{aligned} \tag{10}$$

When:

$$\begin{aligned} &\tau = 0 - 0,\ x_0'^{-} > 0;\ \ \tau = 0 + 0,\ x_0'^{+} = -x_0'^{-} < 0, \\ &\tau = \tau_1 - 0,\ x_1'^{-} < 0;\ \ \tau = \tau_1 + 0,\ x_1'^{+} = -x_1'^{-} > 0. \end{aligned} \tag{11}$$

In the interval:

$$\tau \in \left(\tau = 0 + 0, \tau = \tau_1 - 0\right), \tag{12}$$

the motion takes place:

$$x = C_1 sin\tau + D_1 cos\tau, \tag{13}$$

where according to the initial conditions given by the Eqs. (6), (7):

$$x_s = D_1,\ \ -x_0'^{-} = +C_1, \tag{14}$$

that is:

$$x = -x_0'^{-} sin\tau + x_s cos\tau. \tag{15}$$

At the end of the interval according to the Eqs. (10), (11) from the Eq. (10) it is obtained:

$$-x_s = -x_0'^{-} sin\tau_1 + x_s cos\tau_1, \tag{16}$$

$$x_1'^{-} = -x_0'^{-} cos\tau_1 - x_s sin\tau_1 = -x_0'^{-}. \tag{17}$$

From the Eq. (16):

$$\frac{x_0'^{-}}{x_s} = \frac{1 + cos\tau_1}{sin\tau_1}. \tag{18}$$

The same result is obtained from the Eq. (17).

The eigen period of motion $\bar{\tau}$ and the eigenfrequency $\bar{\omega}$ are:

$$\bar{\tau} = 2\tau_1 = \frac{2\pi}{\bar{\omega}},\ \text{or}\ \frac{\bar{\tau}}{2} = \tau_1 = \frac{\pi}{\bar{\omega}}. \tag{19}$$

From the Eq. (18) it follows that in reality τ_1 is to be greater than 0 and smaller than π, that is:

$$\tau_1 \in \left(> 0, < \pi\right). \tag{20}$$

From the Eqs. (18) and (19):

$$\frac{x_0'^{-}}{x_s} = \frac{1 + cos0.5\bar{\tau}}{sin0.5\bar{\tau}} \text{ and } \frac{x_0'^{-}}{x_s} = \frac{1 + cos\dfrac{\pi}{\bar{\omega}}}{sin\dfrac{\pi}{\bar{\omega}}}, \tag{21}$$

and graphical relationships are obtained $\frac{x_0'^{-}}{x_s}$ as functions of the arguments $\bar{\tau}$ and $\bar{\omega}$ (Fig. 2 and Fig. 3).

Further according to the Eqs. (9) – (11) graphical relationships are calculated $x = x\left(\tau\right)$ and $x' = x'\left(\tau\right)$ and their expansion into Fourier series according to the frequencies $\bar{\omega}$, $2\bar{\omega}$, $3\bar{\omega}$ at several values of $\frac{x_0'^{-}}{x_s}$ is performed.

3.1. Dynamics for different initial velocities

Zero initial displacement and definite position of the impact surface are assumed:

$$x\left(0\right) = 0,\ x_s = -0.749. \tag{22}$$

Results for:

$$x'\left(0\right) = -1 \tag{23}$$

are shown in Fig. 4.

Results for:

$$x'\left(0\right) = -1.25 \tag{24}$$

are shown in Fig. 5.

Results for:

$$x'\left(0\right) = -1.5, \tag{25}$$

are shown in Fig. 6.

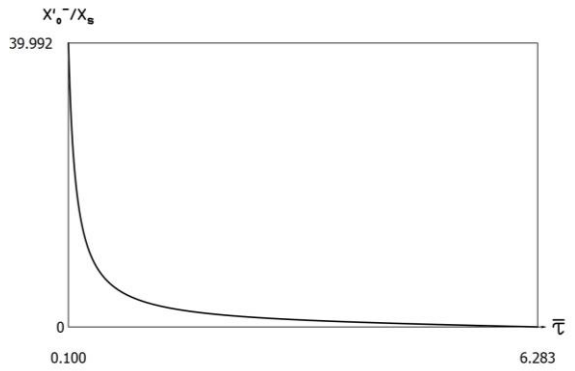

a

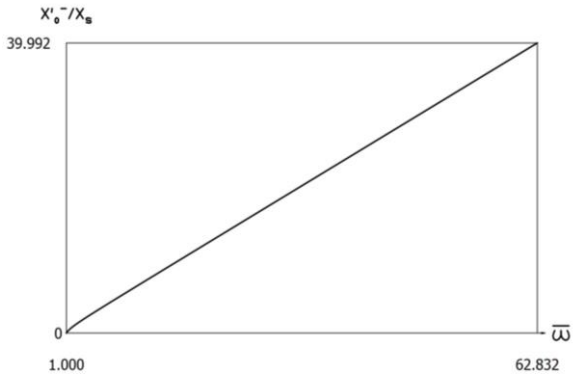

b

Fig. 2 $\frac{x_0'^{-}}{x_s}$ as function of $\bar{\tau}$ and $\bar{\omega}$ when minimum value of $\bar{\tau} = 0.1$

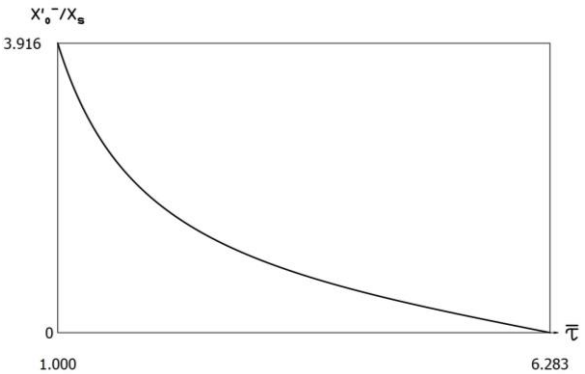

a

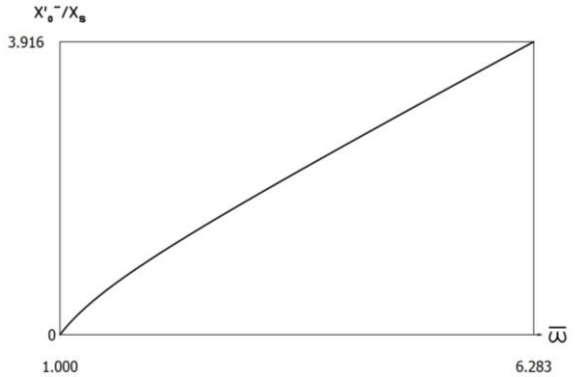

b

Fig. 3 $\frac{x_0'^{-}}{x_s}$ as function of $\bar{\tau}$ and $\bar{\omega}$ when minimum value of $\bar{\tau} = 1$

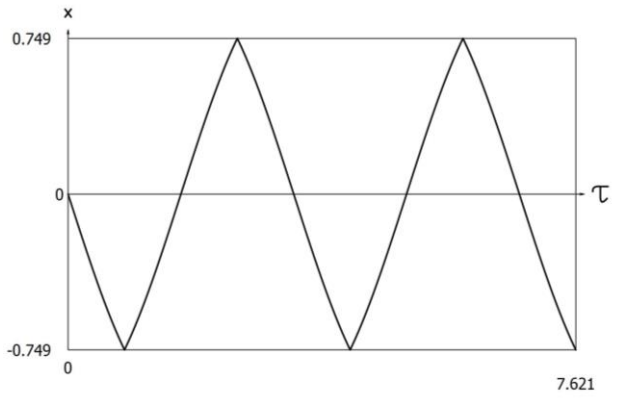

a

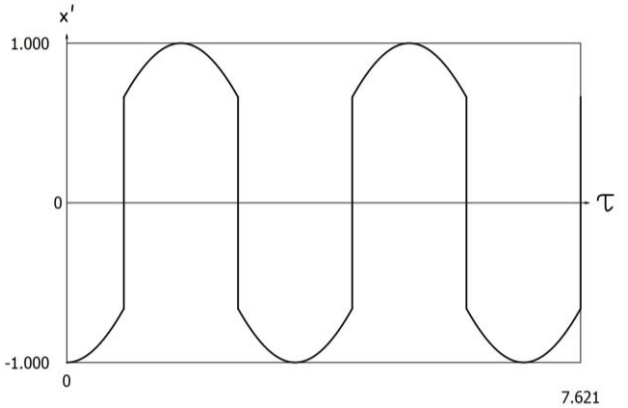

b

Fig. 4 Dynamics of the system for $x'(0) = -1$

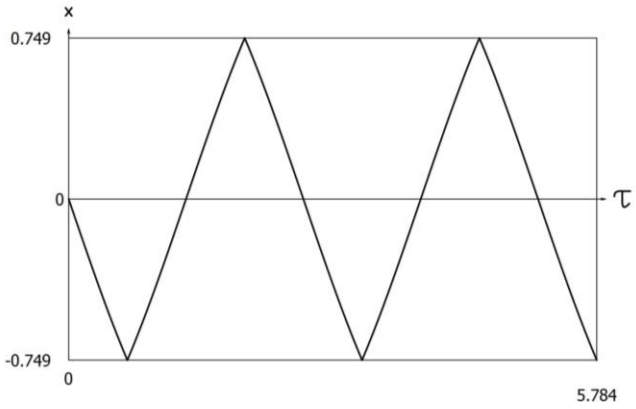

a

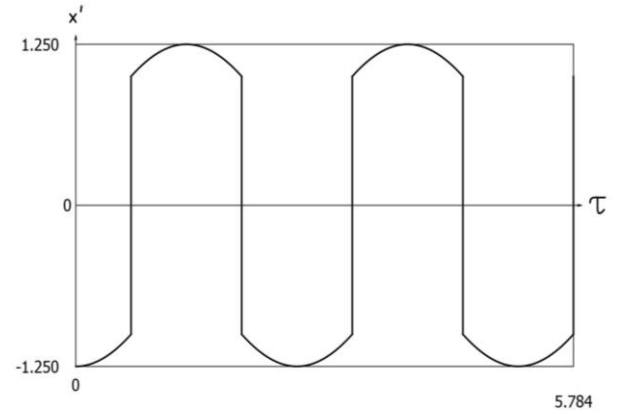

b

Fig. 5 Dynamics of the system for $x'(0) = -1.25$

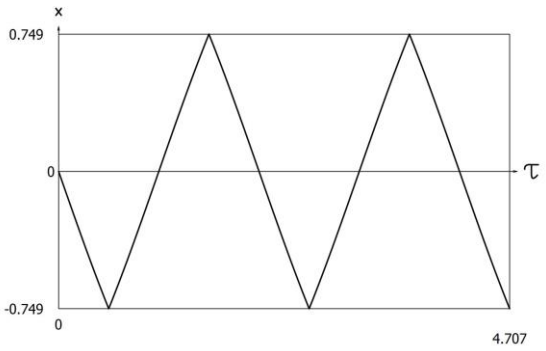

a

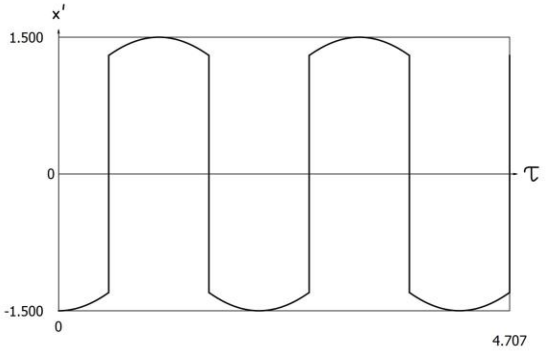

b

Fig. 6 Dynamics of the system for $x'(0) = -1.5$

Dependence of period of vibrations from the initial velocity is shown in Fig. 7. This eigen period or the eigenfrequency determined directly from it has basic influence to the dynamic behavior of the investigated vibrational impact system.

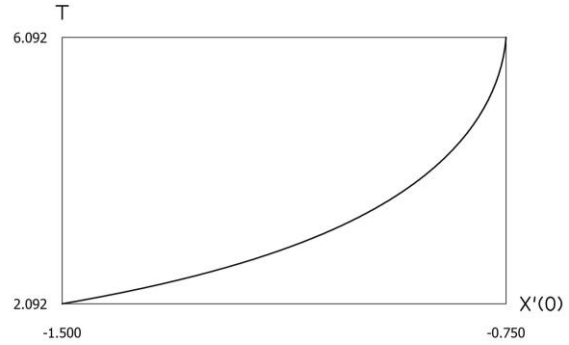

Fig. 7 Dependence of period of vibrations from the initial velocity

The obtained results show the main features of the behavior of the conservative symmetric vibrational impact system.

3.2. Investigation of velocities before and after impacts for various positions of the impact surfaces

Initial conditions are assumed to be:

$$x(0) = 0,\ x'(0) = -1.501. \tag{26}$$

Velocities before impact as functions of the position of symmetric impacting surfaces for the first impacting surface are shown in Fig. 8. Velocities after impact as functions of the position of symmetric impacting surfaces for the first impacting surface are shown in Fig. 9.

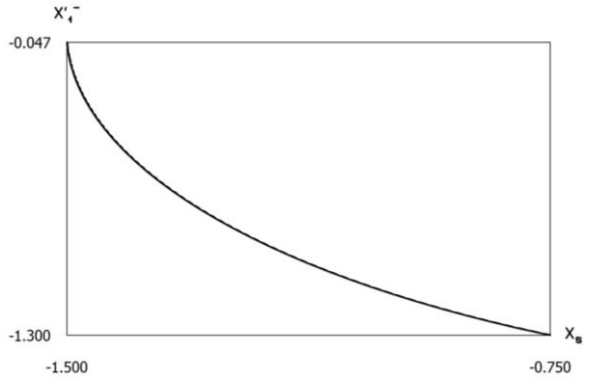

Fig. 8 Velocities before impact as functions of the position of symmetric impacting surfaces for the first impacting surface

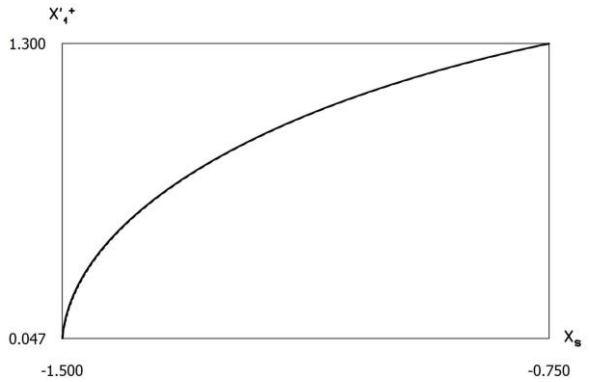

Fig. 9 Velocities after impact as functions of the position of symmetric impacting surfaces for the first impacting surface

Velocities before impact as functions of the position of symmetric impacting surfaces for the second impacting surface are shown in Fig. 10. Velocities after impact as functions of the position of symmetric impacting surfaces for the second impacting surface are shown in Fig. 11.

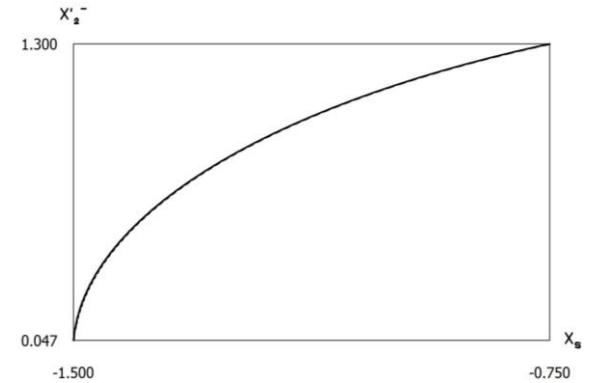

Fig. 10 Velocities before impact as functions of the position of symmetric impacting surfaces for the second impacting surface

The presented graphical relationships of velocities before and after impact for both impacting surfaces show the behavior of the symmetric vibrational impact system.

3.3. Investigation of amplitudes of the first harmonics

It is assumed that:

$$x_s = -0.75. \tag{27}$$

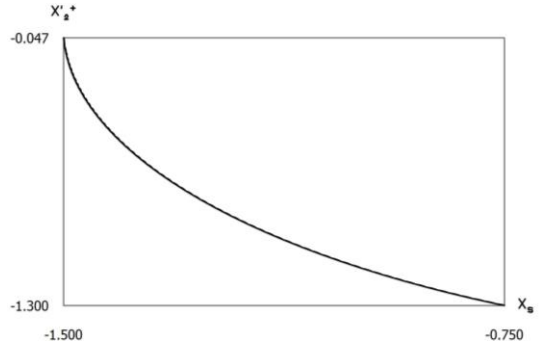

Fig. 11 Velocities after impact as functions of the position of symmetric impacting surfaces for the second impacting surface

Constant part and amplitudes of the first three harmonics of displacement are presented in Fig. 12.

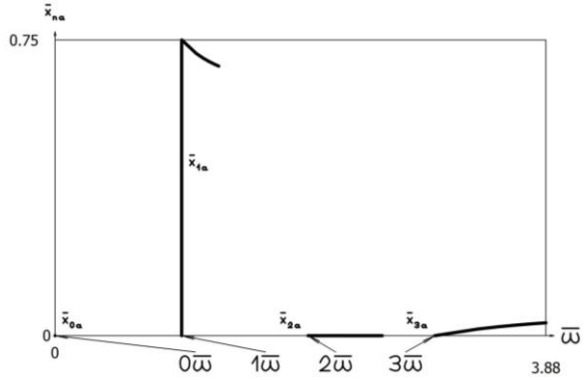

Fig. 12 Constant part and amplitudes of the first three harmonics of displacement

Constant part and amplitudes of the first three harmonics of velocity are presented in Fig. 13.

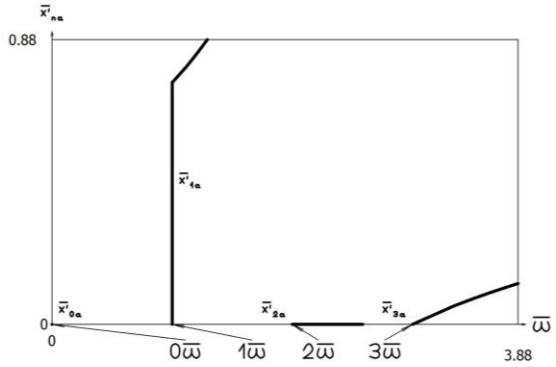

Fig. 13 Constant part and amplitudes of the first three harmonics of velocity

4. Dynamics of the non-conservative system for the case of harmonic excitation

According to the Eqs. (3) – (7) steady state motions are investigated in the vicinities of the resonant frequencies of the conservative system.

It is known that stationary regimes in the vicinities of the frequencies $\bar{\omega}$, $2\bar{\omega}$, $3\bar{\omega}$, … are single valued and have their maximum values according to the velocities of impacts and amplitudes.

The exciting force is assumed as:

$$\bar{f} = f \sin \nu\tau. \tag{28}$$

Zero initial conditions are assumed:

$$x(0) = 0,\ x'(0) = 0. \tag{29}$$

4.1. Dynamics for different coefficients of restitution

The following parameters of the system are assumed:

$$\nu = 1,\ f = -1,\ h = 0.1,\ x_s = -0.5. \tag{30}$$

Results for two typical regimes of motion are presented further.

Results in steady state regime for:

$$R = 0.9, \tag{31}$$

are shown in Fig. 14.

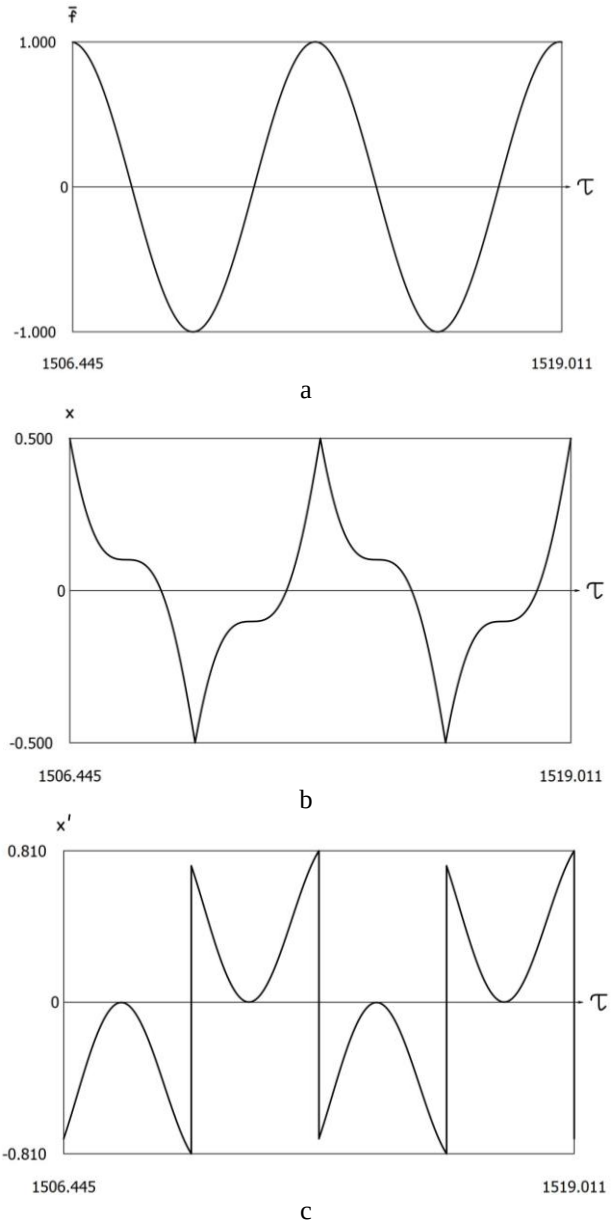

Fig. 14 Dynamics in steady state regime for $\nu = 1,\ f = -1,\ h = 0.1,\ x_s = -0.5,\ R = 0.9$

Results in steady state regime for:

$$R = 0.3, \tag{32}$$

are shown in Fig. 15.

The substantial effect of coefficient of restitution to the dynamics of the system is seen from the presented results.

4.2. Dynamics for different positions of the impact surfaces

The following parameters of the system are assumed:

$$\nu = 1,\ f = -1,\ h = 0.1,\ R = 0.7. \tag{33}$$

Results for four typical regimes of motion are presented further.

Results in steady state regime for:

$$x_s = -0.3, \tag{34}$$

are shown in Fig. 16. From the presented results it is seen that in a period of excitation two impacts to each impacting surface take place.

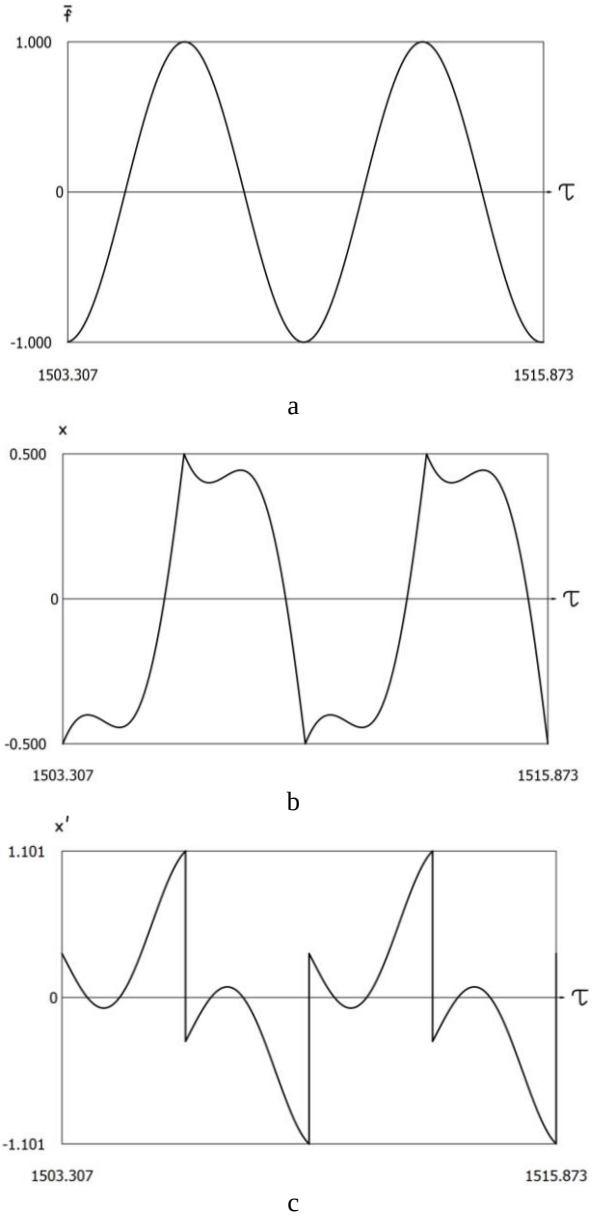

Fig. 15 Dynamics in steady state regime for $\nu = 1,\ f = -1,\ h = 0.1,\ x_s = -0.5,\ R = 0.3$

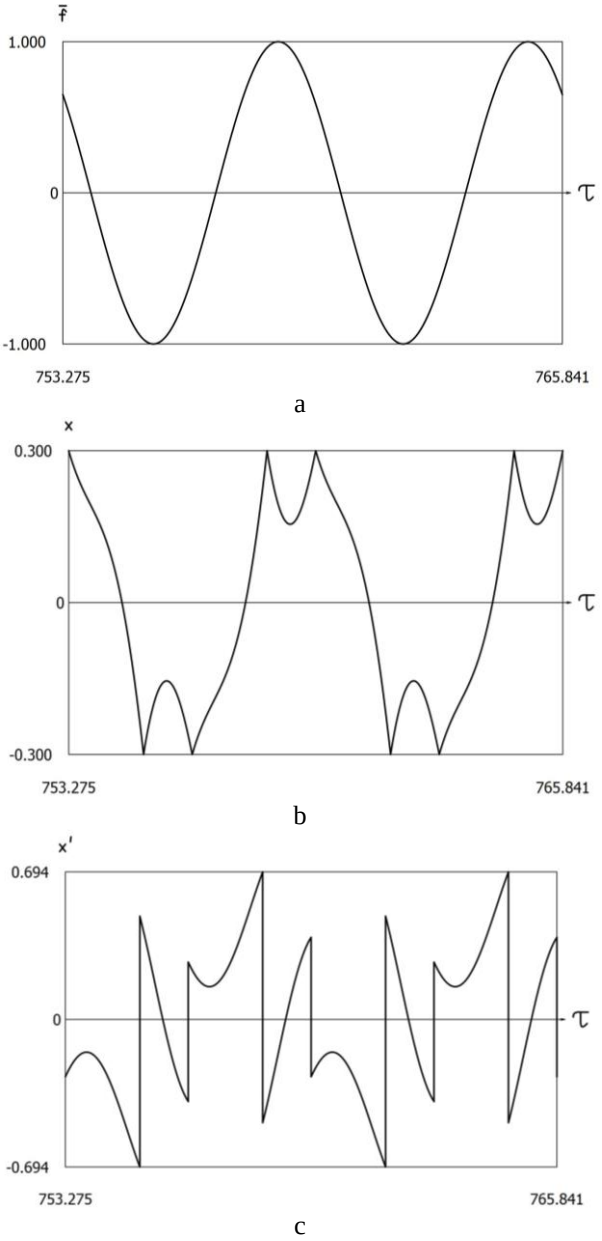

Fig. 16 Dynamics in steady state regime for $\nu = 1,\ f = -1,\ h = 0.1,\ R = 0.7,\ x_s = -0.3$

Results in steady state regime for:

$$x_s = -0.4, \tag{35}$$

are shown in Fig. 17. From the presented results it is seen that in a period of excitation one impact to each impacting surface takes place.

Results in steady state regime for:

$$x_s = -0.5, \tag{36}$$

are shown in Fig. 18. From the presented results it is seen that in a period of excitation one impact to each impacting surface takes place, but character of variation of displacement substantially differs from the previous case.

Results in steady state regime for:

$$x_s = -0.6, \tag{37}$$

are shown in Fig. 19. From the presented results it is seen that in a period of excitation one impact to each impacting surface takes place, but character of variation of displacement differs from both previous cases.

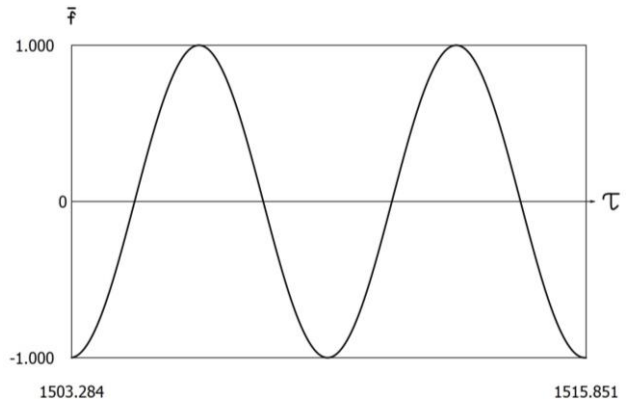

a

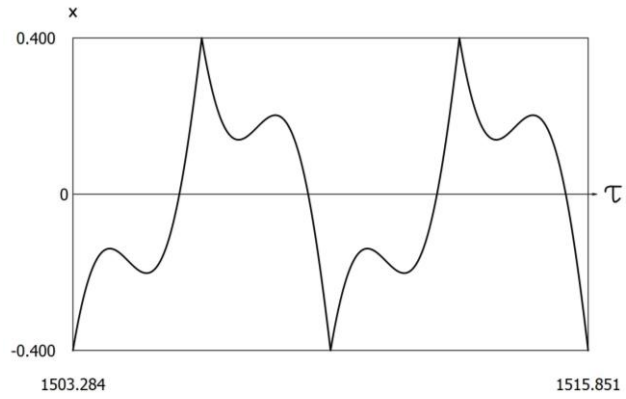

b

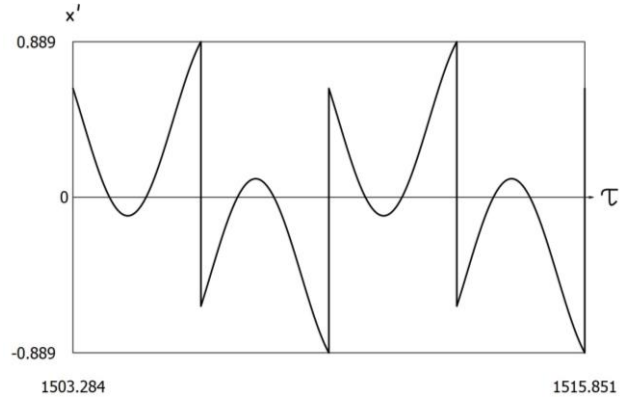

c

Fig. 17 Dynamics in steady state regime for $\nu = 1,\ f = -1,\ h = 0.1,\ R = 0.7,\ x_s = -0.4$

The effect of position of impacting surfaces to the dynamics of the system is seen from the presented graphical results.

4.3. Investigation of minimum and maximum displacements as functions of frequency of excitation

The following parameters of the system are assumed:

$$f = -1,\ h = 0.1,\ R = 0.7. \qquad (38)$$

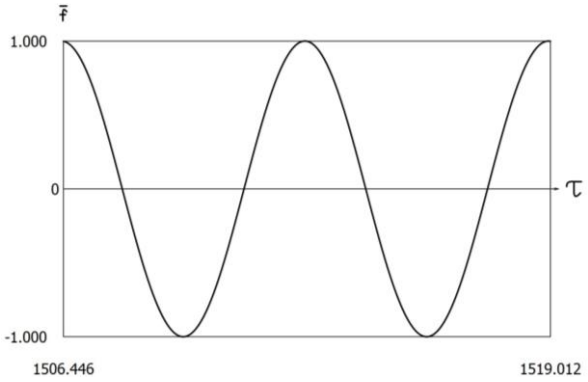

a

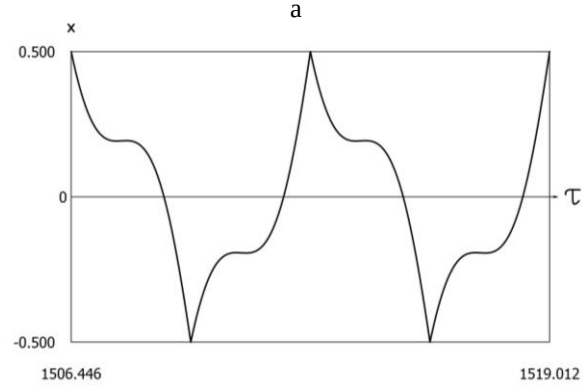

b

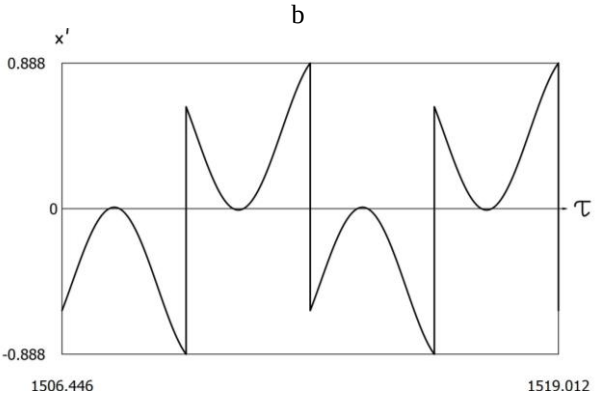

c

Fig. 18 Dynamics in steady state regime for $\nu = 1,\ f = -1,\ h = 0.1,\ R = 0.7,\ x_s = -0.5$

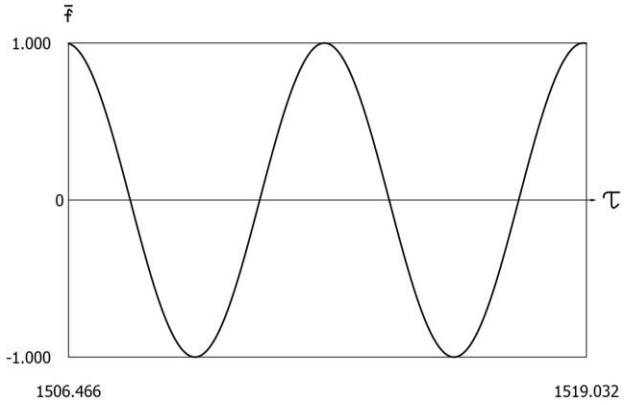

a

Fig. 19 Dynamics in steady state regime for $\nu = 1,\ f = -1,\ h = 0.1,\ R = 0.7,\ x_s = -0.6$

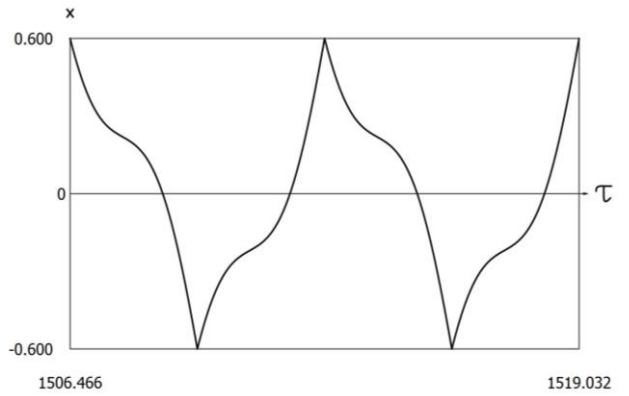

b

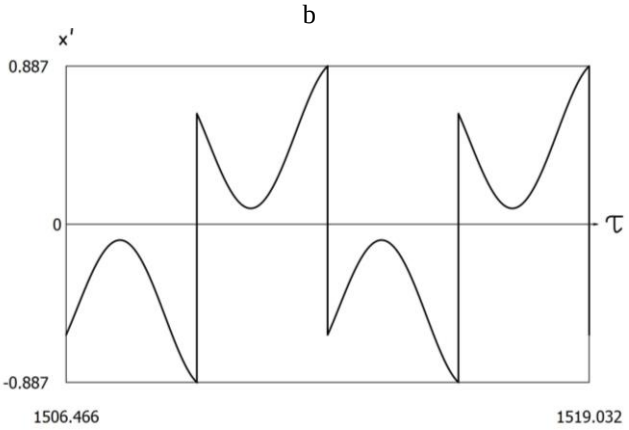

c

Fig. 19 Continuation

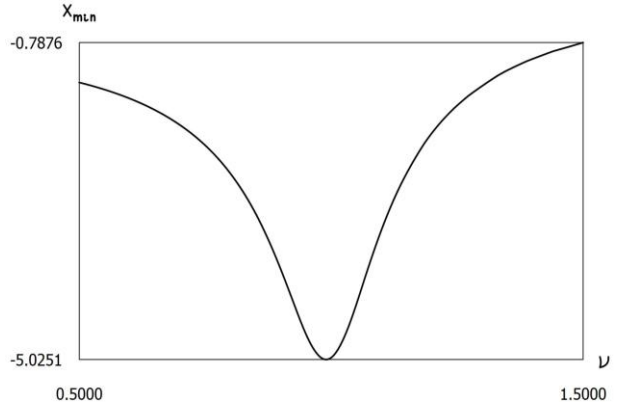

a

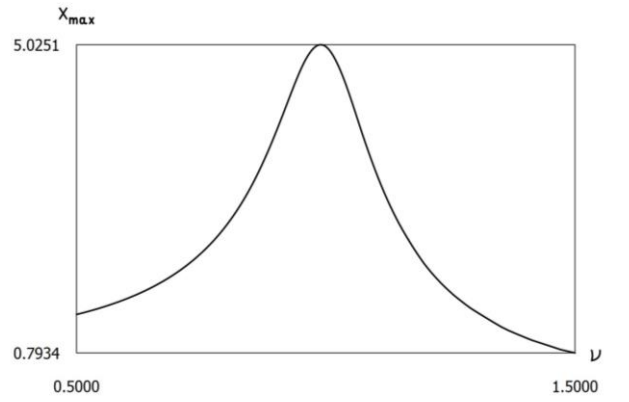

b

Fig. 20 Minimum and maximum displacements in steady state regime for $f=-1,\ h=0.1,\ R=0.7,\ x_s=-6$

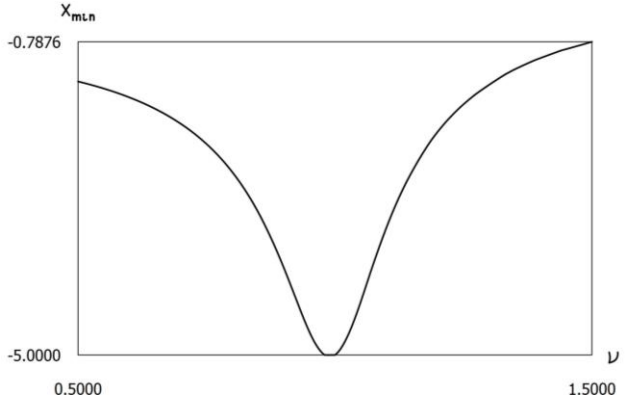

a

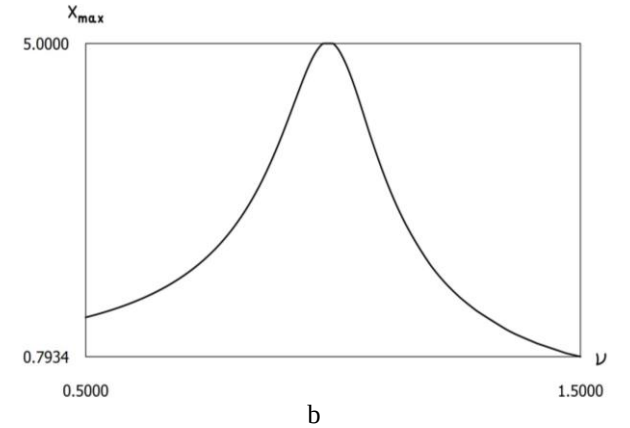

b

Fig. 21 Minimum and maximum displacements in steady state regime for $f=-1,\ h=0.1,\ R=0.7,\ x_s=-5$

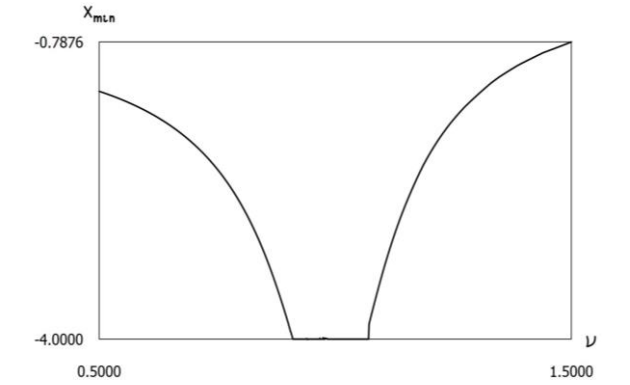

a

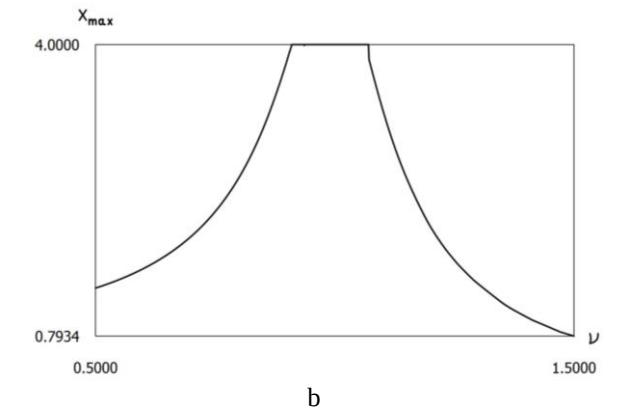

b

Fig. 22 Minimum and maximum displacements in steady state regime for $f=-1,\ h=0.1,\ R=0.7,\ x_s=-4$

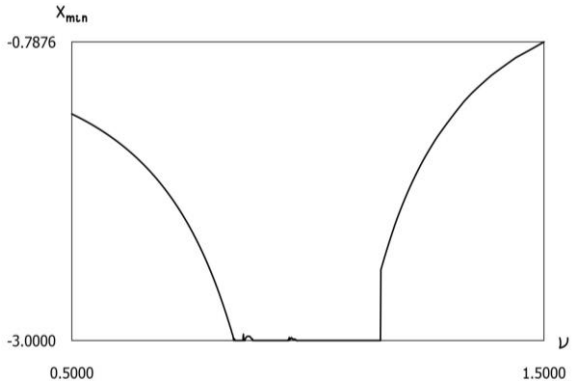

a

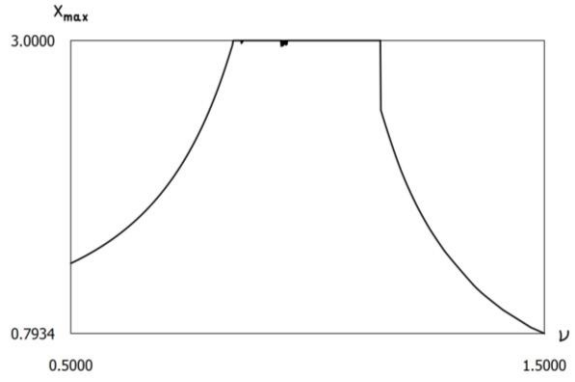

b

Fig. 23 Minimum and maximum displacements in steady state regime for $f = -1,\ h = 0.1,\ R = 0.7,\ x_s = -3$

Results in steady state regime for:

$$x_s = -6, \tag{39}$$

are shown in Fig. 20.

Results in steady state regime for:

$$x_s = -5, \tag{40}$$

are shown in Fig. 21.Results in steady state regime for:

$$x_s = -4, \tag{41}$$

are shown in Fig. 22.

Results in steady state regime for:

$$x_s = -3, \tag{42}$$

are shown in Fig. 23.

The effect of position of impacting surfaces to the dynamics of the system is seen from the presented graphical results.

5. Conclusions

In the field of vibrational impact systems important results of investigations have been obtained, which became widely accepted and are applied in further investigations. Contemporary investigations of systems of new type with specific nonlinearities as well as with motions of chaotic type are performed.

In some types of nonlinear systems between the hard and soft zones of excitation of vibrations optimal regimes according to the shape of motion exist. Here this fact is generalized for the vibrator with two symmetric impacting pairs of elements.

According to the model of the system free vibrations of the system and their parameters are determined as well as forced harmonic vibrations and their specific features are determined.

Dynamics for different initial velocities is investigated. Dependence of period of vibrations from the initial velocity is determined. This eigen period or the eigenfrequency determined directly from it has basic influence to the dynamic behavior of the investigated vibrational impact system. The obtained results show the main features of the behavior of the conservative symmetric vibrational impact system.

Investigation of velocities before and after impacts for various positions of the impact surfaces is performed. The presented graphical relationships of velocities before and after impact for both impacting surfaces show the behavior of the symmetric vibrational impact system.

Investigation of the system with dissipation of energy for the case of harmonic excitation is performed. Stationary regimes in the vicinities of the eigenfrequencies are single valued and have their maximum values according to the velocities of impacts and amplitudes.

Dynamics for different coefficients of restitution is investigated. Results for two typical regimes of motion are presented. The substantial effect of coefficient of restitution to the dynamics of the system is seen from the presented results.

Dynamics for different positions of the impact surfaces is investigated. Results for four typical regimes of motion are presented. For the first set of parameters, it is seen that in a period of excitation two impacts to each impacting surface take place. For the second set of parameters, it is seen that in a period of excitation one impact to each impacting surface takes place. For the third set of parameters, it is seen that in a period of excitation one impact to each impacting surface takes place, but character of variation of displacement substantially differs from the previous case. For the fourth set of parameters, it is seen that in a period of excitation one impact to each impacting surface takes place, but character of variation of displacement differs from both previous cases. The effect of position of impacting surfaces to the dynamics of the system is seen from the presented graphical results.

Recommendations for practical applications are provided.

References

1. **Glazunov, V.** 2018. New Mechanisms in Contemporary Robot Engineering. Moscow: Tehnosphere (in Russian).
2. **Ragulskis, K.; Bogdevičius, M.; Mištinas, V.** 2008. Behaviour of dynamic processes in self-exciting vibration of a pipe robot, Journal of Vibroengineering 10(3): 397-399.
3. **Ragulskis, K.; Ragulskis, L.** 2019. Vibroimpact mechanism in one separate case, Mathematical Models in Engineering 5(2): 56-63. https://doi.org/10.21595/mme.2019.20818.

4. **Ragulskienė, V.** 1974. Vibro-Shock Systems (Theory and Applications). Vilnius: Mintis (in Russian).
5. **Kurila, R.; Ragulskienė, V.** 1986. Two-Dimensional Vibro-Transmissions. Vilnius: Mokslas (in Russian).
6. **Ragulskis, K.; Bansevičius, R.; Barauskas, R.; Kulvietis, G.** 1987. Vibromotors for Precision Micro-robots. New York: Hemisphere.
7. **Wedig, W. V.** 2016. New resonances and velocity jumps in nonlinear road-vehicle dynamics, Procedia IUTAM 19: 209-218. https://doi.org/10.1016/j.piutam.2016.03.027.
8. **Li, T.; Gourc, E.; Seguy, S.; Berlioz, A.** 2017. Dynamics of two vibro-impact nonlinear energy sinks in parallel under periodic and transient excitations, International Journal of Non-Linear Mechanics 90: 100-110. https://doi.org/10.1016/j.ijnonlinmec.2017.01.010.
9. **Zaitsev, V. A.** 2016. Global asymptotic stabilization of periodic nonlinear systems with stable free dynamics, Systems & Control Letters 91: 7-13. https://doi.org/10.1016/j.sysconle.2016.01.004.
10. **Dankowicz, H.; Fotsch, E.** 2017. On the analysis of chatter in mechanical systems with impacts, Procedia IUTAM 20: 18-25. https://doi.org/10.1016/j.piutam.2017.03.004.
11. **Spedicato, S.; Notarstefano, G.** 2017. An optimal control approach to the design of periodic orbits for mechanical systems with impacts, Nonlinear Analysis: Hybrid Systems 23: 111-121. https://doi.org/10.1016/j.nahs.2016.08.009.
12. **Li, W.; Wierschem, N. E.; Li, X.; Yang, T.** 2018. On the energy transfer mechanism of the single-sided vibro-impact nonlinear energy sink, Journal of Sound and Vibration 437: 166-179. https://doi.org/10.1016/j.jsv.2018.08.057.
13. **Marshall, J. S.** 2018. Modeling and sensitivity analysis of particle impact with a wall with integrated damping mechanisms, Powder Technology 339: 17-24. https://doi.org/10.1016/j.powtec.2018.07.097.
14. **Salahshoor, E.; Ebrahimi, S.; Zhang, Y.** 2018. Frequency analysis of a typical planar flexible multibody system with joint clearances, Mechanism and Machine Theory 126: 429-456. https://doi.org/10.1016/j.mechmachtheory.2018.04.027.
15. **Starossek, U.** 2016. Forced response of low-frequency pendulum mechanism, Mechanism and Machine Theory 99: 207-216. https://doi.org/10.1016/j.mechmachtheory.2016.01.004.
16. **Wang, S.; Hua, L.; Yang, C.; Zhang, Y.; Tan, X.** 2018. Nonlinear vibrations of a piecewise-linear quarter-car truck model by incremental harmonic balance method, Nonlinear Dynamics 92: 1719-1732. https://doi.org/10.1007/s11071-018-4157-6.
17. **Alevras, P.; Theodossiades, S.; Rahnejat, H.** 2018. On the dynamics of a nonlinear energy harvester with multiple resonant zones, Nonlinear Dynamics 92: 1271-1286. https://doi.org/10.1007/s11071-018-4124-2.
18. **Sinha, A.; Bharti, S. K.; Samantaray, A. K.; Chakraborty, G.; Bhattacharyya, R.** 2018. Sommerfeld effect in an oscillator with a reciprocating mass, Nonlinear Dynamics 93: 1719-1739. https://doi.org/10.1007/s11071-018-4287-x.
19. **Habib, G.; Cirillo, G. I.; Kerschen, G.** 2018. Isolated resonances and nonlinear damping, Nonlinear Dynamics 93: 979-994. https://doi.org/10.1007/s11071-018-4240-z.

Kazimieras RAGULSKIS, Liutauras RAGULSKIS

VIBRATION DRIVES WITH TWO IMPACTING PAIRS FOR PRECISE ROBOTS

S u m m a r y

Such robots, when they consist of two separate sequentially connected robots, are of high precision. The first part – robot is not of a high precision adjusted to perform comparatively large displacements, while the second part – robot is meant to perform comparatively small displacements with very high precision if compared with the first part. Motors of all the motions are of vibrational type.

First of all, vibrators of vibrational impact type with impacts of rigid bodies are investigated.

Earlier it was shown that in some types of nonlinear systems between the hard and soft zones of excitation of vibrations optimal regimes according to the shape of motion exist. Here this fact is generalized for the vibrator with two symmetric impacting pairs of elements. According to the model of the system free vibrations of the system and their parameters are determined as well as forced harmonic vibrations and their specific features are determined. Recommendations for practical applications are provided.

Keywords: precise robots, vibrator, two impacting pairs, nonlinear system, eigen vibrations, optimal regimes.

Received September 13, 2022
Accepted April 5, 2023